Journal of Sound and Vibration (1999) **228**(4), 717–730
Article No. jsvi.1999.2448, available online at http://www.idealibrary.com on IDEAL®

PARAMETERIZATION OF DAMAGE IN REINFORCED CONCRETE STRUCTURES USING MODEL UPDATING

M. M. ABDEL WAHAB

School of Mechanical & Materials Engineering, University of Surrey, Guildford, GU2 5XH, England

AND

G. DE ROECK AND B. PEETERS

Department of Civil Engineering, Katholieke Universiteit te Leuven, Belgium

(*Received* 7 *January* 1999, *and in final form* 14 *May* 1999)

This paper describes the application of finite element model updating to reinforced concrete beams in order to detect and quantify damage. Three simply supported beams are considered in this study: two of them are subjected to a single concentrated load while the third one to two concentrated loads. The static loading system is applied in different steps up to failure so that dynamic measurements can be carried out after each load step. The measured modal parameters are used afterwards to update a finite element model in order to localize and to quantify the damage. The updating algorithm is based on the sensitivity approach in which the discrepancies between the analytical and experimental modal data are minimized in an iterative manner. A new concept for damage parametrization is introduced. A damage function characterized by three parameters is proposed. In such a function, only three parameters are used to describe the damage pattern of the reinforced concrete beams. These parameters are related to the bending stiffness of the beams and updated so that the measured natural frequencies are reproduced. The results demonstrate the efficiency of the proposed technique to quantify the damage pattern.

1. INTRODUCTION

The research effort to use changes in modal parameters to detect and quantify structural damage in civil engineering constructions has been increased during the last decade. Since the modal parameters are affected by the stiffness, they can be used to monitor the structural integrity. Depending on the location and severity of damage, changes of modal parameters, especially natural frequencies and mode shapes, may be different from one mode of vibration to another. This fact implies that modal data are good candidates to localize damage qualitative as well as quantitative. The main advantage of using vibration monitoring as a damage indicator tool is due to its simplicity and cheapness. The dynamic responses of the structure due to artificial excitation or ambient vibration in the service condition

0022-460X/99/490717 + 14 $30.00/0

are recorded by means of sensors, mostly accelerometers. The modal parameters can be extracted from the measured responses using time or frequency domain techniques.

Damage detection using changes in modal data can be classified into two broad categories. The first category is the "response-based approach" in which the loss in stiffness is directly related to the measured modal parameters. Cawley and Adams [1] proposed a method based on the assumption that the ratio of frequency changes in two modes is related to the location of damage. In this method, theoretical frequency ratios due to damage at different positions on the structure are compared to the measured ones. Salawu [2] has introduced a global integrity index for detecting damage using a linear combination of the frequencies of both damaged and intact structure. Uzgider *et al.* [3] have used a technique based on identification of some stiffness parameters by using measured natural frequencies. In this method, vibration modes for which the stiffness parameters are mostly sensitive are selected and used to evaluate the magnitude of these parameters. Other applications of the "response-based approach" are due to Zhang *et al.* [4, 5] for detecting structural faults in frame structures and localizing defects in foundation piles. The drawback of most of the methods based on the above approach is that consideration of all possible damage scenarios at different locations on the structure is required. Consequently, excessive computational time is needed especially for large structures.

The second category of damage detection techniques is the "model-based approach" that is based on updating certain parameters to get a perfect agreement between the experimentally measured modal parameters and a finite element model. The updated parameters can be interpreted afterwards to evaluate damage and identify its location. Mottershead and James [6] have used an updating technique to correct the mass and stiffness at the joint of an aluminium space frame. Abdel Wahab *et al.* [7] were able to determine the percentage reduction in bending stiffness of a damaged reinforced concrete beam using model updating. Collins *et al.* [8, 9] have proposed an updating method based on a statistical technique. The updated parameters are estimated so that their variance is minimum. Friswell [10] has adopted the minimum variance method of Collins *et al.* [8, 9] assuming that the measurement noise and the parameter estimates are not independent. Grossman [11] has used a penalty function method based on a weighted average of the ratio between the measured and analytical modal data. From a theoretical viewpoint, natural frequencies as well as mode shapes can be used as modal parameters in the updating algorithm. However, in practice the measured mode shapes are normally less accurate than the natural frequencies. Up to 20% measurement error in the eigenvectors may be expected [12]. On the contrary, the error in the measured natural frequencies is around 1%. Therefore, the eigenvalues can be used with more confidence than the eigenvectors in the updating procedure. If the quality of the measured mode shapes improves, they can contribute to the updating algorithm more efficiently. Recently, a scanning laser Doppler measurement system [13, 14] has been developed in order to improve the quality of the measured mode shapes.

Application of the damage detection method using modal data to concrete structures, such as bridges, has been reported in the literature by many researches, e.g., Salawu [15], Williams and Salawu [16], Sikorsky and Stubbs [17], Farrar and Jauregai [18], Ventura Adebar [19], Krishnan *et al.* [20] and Abdel Wahab *et al.* [21].

This paper deals with the model-based approach and its application to three laboratory reinforced concrete beams. The first two beams are subjected to a single concentrated load in the middle while the third one to two concentrated loads at one-third and two-thirds of the beam length. All three beams are loaded statically in different steps until plastic failure. After each load step, the dynamic responses of the beams are recorded at different points distributed over the beam length due to hammer excitation. A time domain system identification technique is applied to the measured responses to extract the modal parameters. An updating algorithm is developed and applied at the different damage stages in order to determine the variation of the reduction in bending stiffness along the beam length. The damage pattern is characterized by using a so-called damage function. In this function, only three parameters are used to completely describe the damaged zone. These three parameters define the bending stiffness along the beam length. In the following sections, first the updating algorithm is briefly reviewed. Next, the reinforced concrete beams and the experimental set-up are presented. Then, the proposed damage function is described. Finally, results are reported and discussed.

2. UPDATING ALGORITHM

The method is based on minimizing the difference between measured and calculated modal parameters. The resulting least-squares problem is solved by the Gauss–Newton method. Practical implementation of the Gauss–Newton methods relies upon the application of the singular value decomposition [22]. The Gauss–Newton equation is similar to the truncated Taylor series used in the penalty function method [23]. The penalty function equation can be written in the following form:

$$\mathbf{S}\delta\boldsymbol{\theta} - \delta\mathbf{z} = \mathbf{0}, \tag{1}$$

where $\delta\mathbf{z}$ is the discrepancy between the measured modal data and the finite element solution. $\delta\boldsymbol{\theta}$ is the perturbation in the unknown parameters to be updated. $\mathbf{S}$ is the Jacobian or sensitivity matrix containing the first derivative of the calculated modal parameters ($\mathbf{z}$) with respect to the unknown parameters ($\boldsymbol{\theta}$). Equation (1) can be written as

$$[\mathbf{z}_m - \mathbf{z}_j]_{n\times 1} = [\mathbf{S}_j]_{n\times p}[\boldsymbol{\theta}_{j+1} - \boldsymbol{\theta}_j]_{p\times 1}, \tag{2}$$

where $\mathbf{z}_m$ represents the measured modal parameters used in the updating algorithm. The subscript "j" indicates the iteration number at which the sensitivity matrix is computed. The number of modal parameters (e.g., eigenfrequencies, mode shapes and/or modal curvatures) is equal to n, while p is the number of unknown parameters to be updated. The sensitivity matrix is seldom square because the number of modal parameters is not necessary equal to that of unknown parameters.

To be able to compute $\boldsymbol{\theta}_{j+1}$ from equation (2), the inverse of the matrix $\mathbf{S}_j$ should be calculated. If $\mathbf{S}$ is not square, then the inverse of $\mathbf{S}$ does not exist and the pseudo-inverse, S^t, is used. The pseudo-inverse can be calculated by solving the singular value decomposition of $\mathbf{S}$ [23]. The solution of equation (2) is then

$$[\boldsymbol{\theta}_{j+1}]_{p\times 1} = [\boldsymbol{\theta}_j]_{p\times 1} + [\mathbf{S}_j^t]_{p\times n}[\mathbf{z}_m - \mathbf{z}_j]_{n\times 1}. \tag{3}$$

In equation (3), it is assumed that the measured data are equally weighted. The lower frequencies are in general more accurately determined than the higher ones. Therefore, in the updating algorithm the lower natural frequencies are given more weight than the higher. The sensitivity matrix, $\mathbf{S}$, is defined as the first derivative of the modal-parameters ($\mathbf{z}$) with respect to the unknown parameters ($\boldsymbol{\theta}$). A finite difference approximation is used to calculate the elements of the sensitivity matrix. Each column of the sensitivity matrix is computed from two finite element analyses for two $\boldsymbol{\theta}$ values differing by an incremental amount $\Delta\boldsymbol{\theta}$. A 10% incremental value has been chosen and implemented in the updating algorithm. The algorithm has been also tested using different incremental values between 1 and 10%. No difference in results has been observed. The use of the finite difference approximation provides usually gradients with acceptable accuracy especially when the gradient is not small [22].

3. DESCRIPTION OF BEAMS

All three beams are designed in the same way. A length of 6 m and cross-section of 20 × 25 cm reinforced with six steel bars of diameter 16 mm as shown in Figure 1 are chosen. Vertical stirrups of 8 mm diameter are equally distributed along the beam length every 200 mm. The dimensions of the beams are selected so that the first resonant frequency should lie within the frequency range of typical civil engineering structures. The chosen dimensions produce a first resonant frequency is about 20 Hz. The reinforcement ratio is 1·4%, which allows for a plastic failure at

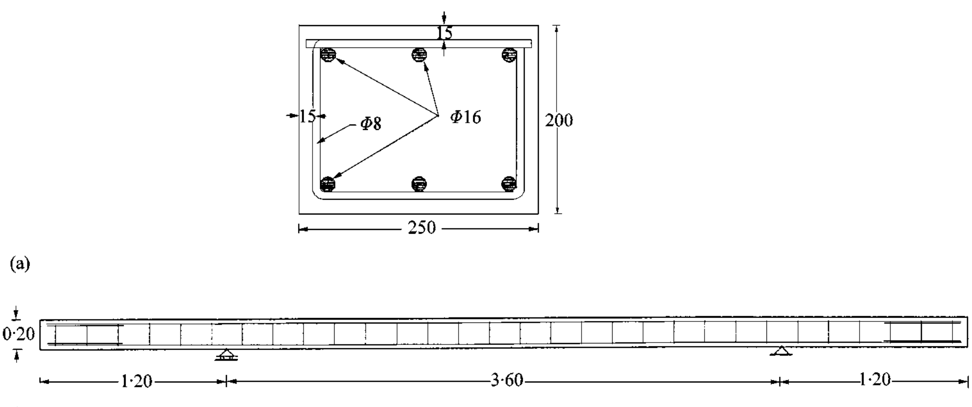

Figure 1. Beam geometry. (a) Cross-section (dimensions in mm); (b) Elevation (dimensions in m).

a total load value of about 60 kN so that different load steps can be performed. The vertical stirrups ensure that bending failure takes place.

4. EXPERIMENTAL SET-UP

For the static test configuration, the beams are simply supported on one hinge and one roller support. For beam 1 and 2, the distance between the two supports is 3·6 m leaving two cantilevers each of 1·2 m at both sides of the beam. The load is applied in the middle of the beam and the deflections at 8 points distributed over the beam length are registered as shown in Figure 2. For beam 3, the span is almost equal to the total length of the beam. About 15 cm is left between each support and the edge of the beam. Two concentrated loads are applied at one-third and two-third of the beam length. The deflections are measured at 9 points. Figure 3 shows the static test configuration for beam 3. Different load steps are considered for each beam. Table 1 summarizes the load level at each step for the three beams.

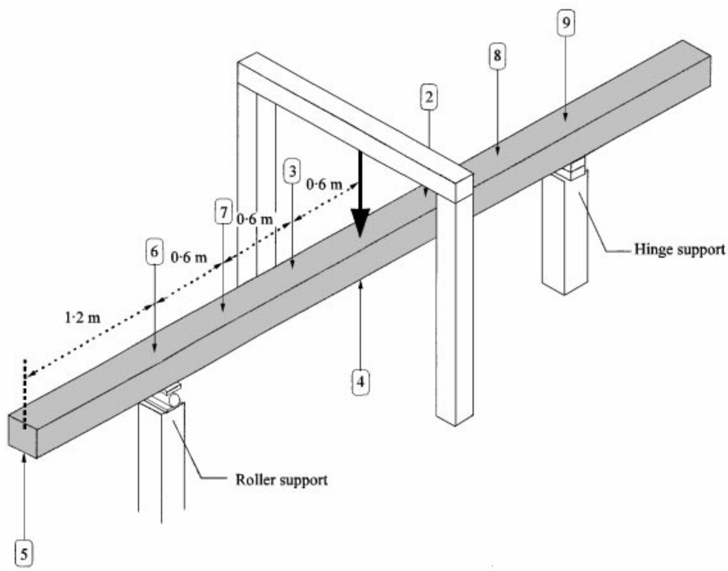

Figure 2. Static test configuration for beams 1 and 2. ↓ Hydraulic jack; Displacement transducer.

TABLE 1

Static load steps

	Load step number						
Load (kN)	1	2	3	4	5	6	7
Beam 1	15·5	24·7	32·6	40·2	45·9	60·5	
Beam 2	8	15	24	32	40	50	56
Beam 3	4	6	12	18	24	26	

The value given in Table 1 for beam 3 is the load at each hydraulic jack (see Figure 3).

After each load step, dynamic measurements were carried out. To avoid the influence of not well-defined boundary conditions on the modal parameters a free–free dynamic test set-up designed. The beams are hanged using flexible springs as shown in Figure 4, and excited by means of an impulse hammer (PCB

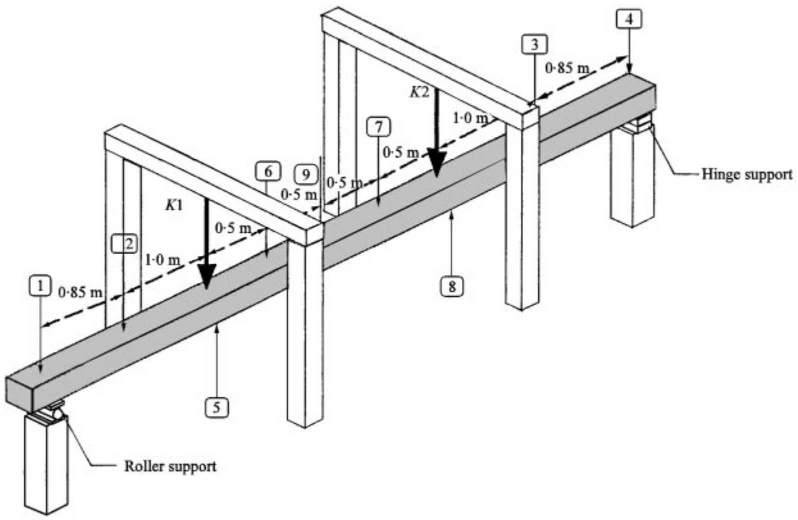

Figure 3. Static test configuration for beam 3. Hydraulic jack; Displacement transducer.

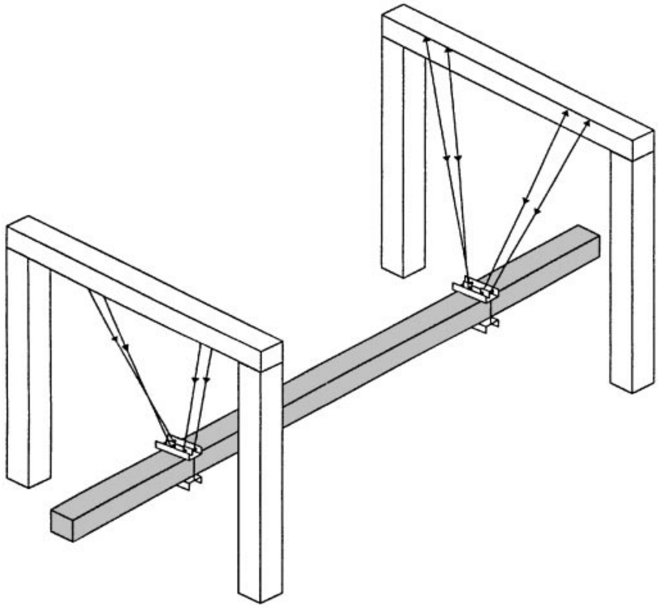

Figure 4. Dynamic test configuration.

GK291B20). The responses are measured at every 20 cm on both sides of the beams using accelerometers PCB 338A35 and 338B35. A total of 62 responses in the vertical direction are registered. The measurement is divided into seven series. Each series contains the data of 8 measured points, the input force and two reference points. For each series, three hammer impact tests are performed. The hammer tip used to excite the beam was chosen to generate frequencies up to 1000 Hz. The data was sampled at 5000 Hz during the measurements. Before applying a system identification frequency, the data was firstly pre-processed: the accelerations are derived from the electrical signal (V) using the accelerometers sensitivities and the data are filtered by a digital low pass filter (8th order Chebyshev type I, with a cut-off frequency of 1000 Hz) and resampled at 2500 Hz. The modal parameters of the beams, i.e., natural frequencies, damping ratios and mode shapes are extracted from the measured data using a time-domain technique. The method is based on the development of a representative linear mathematical model of a dynamic system directly from the observed time-series data. The resulting model, which provides an optimum representation of the system, can then be used to extract the required dynamic parameters. The theoretical background of the method is beyond the scope of this paper and can be found elsewhere [24, 25].

5. DAMAGE FUNCTION

In order to detect damage along the beam length using model updating, one possibility is to update the bending stiffness (EI) of each element in the finite element model. This means that a large number of updating parameters is required to properly describe the variation of the bending stiffness along the beam length. Consequently, a considerable amount of computational time is needed to calculate the sensitivity matrix. Besides, due to measurement and/or discretization errors realistic damage pattern is not always guaranteed if the bending stiffness of each element can vary independently. We are seeking a function that can describe a damage pattern by only a few representative parameters. This function should have the flexibility to represent small as well as large damage zones. Assuming that the reduction in the bending stiffness (EI) can be simulated by a reduction in the E-modulus, the following function is proposed:

$$
\begin{aligned}
&E = E_0[1-(1-\alpha)\cos^2 t] \quad \text{with } t = \frac{\pi}{2}\left(\frac{x}{\beta L/2}\right)^n \quad \text{for } 0 \prec x \prec \beta L/2 \\
&E = E_0 \quad \text{for } \beta L/2 \leqslant x \leqslant L/2,
\end{aligned} \tag{4}
$$

where β, α and n are the damage parameters. L is the beam length and x is the distance along the beam measured from the centre line. A sketch of the proposed function is shown in Figure 5. The parameter β characterizes the length of the damaged zone. It lies in the range between 0 and 1. If β becomes small, a very local damage at the middle of the beam is obtained, while if β is equal to 1, the beam is damaged over its whole length. α characterizes the magnitude of damage. It lies also between 0 and 1. If α is equal to 1, no damage is presented, whereas if α drops to zero, the bending stiffness will vanish at the middle of the beam. The third

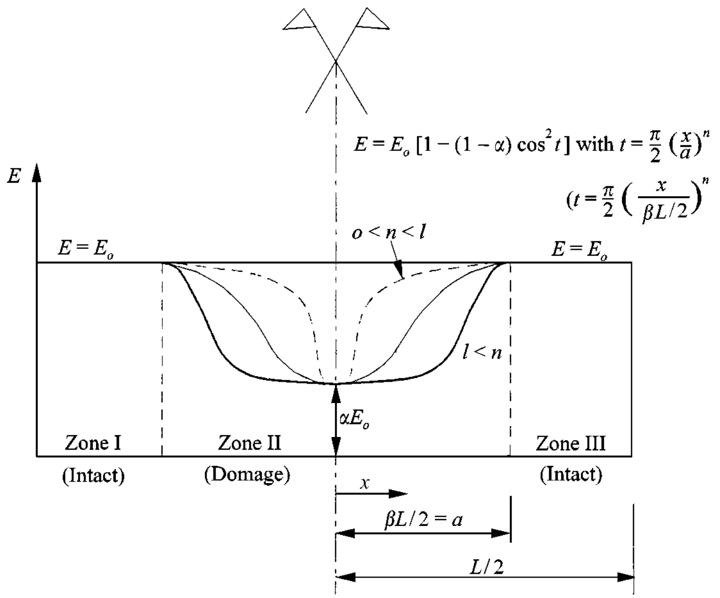

Figure 5. Symmetric damage function.

parameter is the power n that characterizes the variation of the E-modulus from the centre of the beam ($x = 0$) to the end of the damaged zone ($x = \beta L/2$). If n is larger than 1, a flat damage pattern is produced, otherwise a steep pattern is obtained.

By using this proposed function, not only the updating parameters are reduced to three parameters but also a realistic damage pattern is always guaranteed. It should be noted that a symmetric damage pattern is assumed since in the present application all three beams are loaded symmetrically at the middle of the beam. This assumption reduces the number of parameters needed to be updated. However, it is possible to account for non-symmetric damage pattern by assuming two different stiffness variations at the left- and the right-hand side of the centreline of the beam. In such a case, the number of updating parameters will be increased from 3 to 6 parameters (α, (β_1, n_1) for the left-hand side (β_2, n_2) for the right-hand side and a parameter γ that localizes the most severe damage position). The non-symmetric damage function has the following form:

$$E = E_0[1-(1-\alpha_b)\cos^2 t] \quad \text{with } t = \frac{\pi}{2}\left(\frac{x_2}{1-\gamma)\beta_2 L}\right)^{n_2} \quad \text{for the right-hand side,}$$

$$t = \frac{\pi}{2}\left(\frac{x_1}{\gamma\beta_1 L}\right)^{n_1} \quad \text{for the left-hand side,} \tag{5}$$

where β_1, β_2, α_b, n_1 and n_2 are the damage parameter. x_1 and x_2 are the distances along the length L measured from the most damaged position. A sketch of the proposed function is shown in Figure 6. The parameters β_1 and β_2 characterize the length of the damaged zone at left and right of the most damaged position.

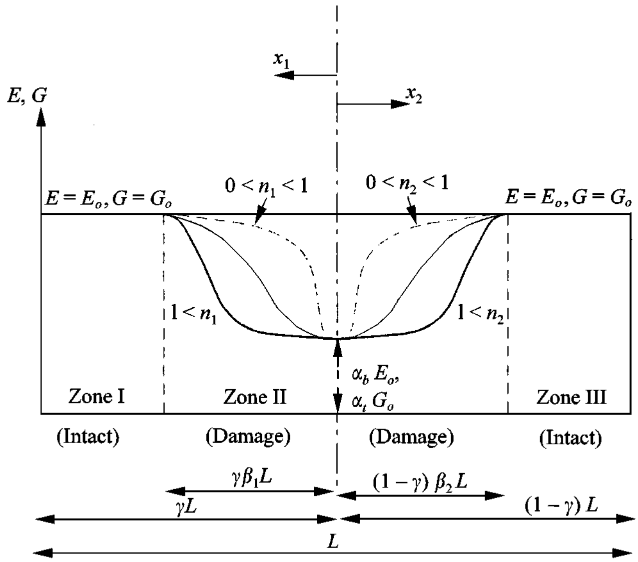

Figure 6. Non-symmetric damage function.

The parameter γ localizes the most damaged section. If α_b is equal to 1, no reduction in EI is presented, whereas if α drops to zero, the bending stiffness will vanish at $x_1 = x_2 = 0$. The parameters n_1 and n_2 characterize the variation of the E-modulus from $x_1 = x_2 = 0$ to the end of the damaged zone at left and right.

It should be noted that in transferring the damage function to the finite element model, β is used to calculate the number of elements over which the damage function should be described. This number is computed as the nearest integer to β times the half of the total number of elements.

6. RESULTS

Before applying any static load to the beams, a dynamic test is performed. This test serves as a reference for later comparison at the different damage stages. A finite element model containing 30 beam elements is constructed. The results of this initial model are fitted in a global way to the reference test results. This can be done by either updating the E-modulus or the density of the whole beam. In Tables 2–4, the measured natural frequencies for the first four bending modes are given for the reference test of each beam and compared to the finite element results. The density is kept the same for all beams and the E-modulus is adopted to give the best agreement with the test results. This assumption is of minor importance since the main goal is to determine the relative reduction in the bending stiffness at the different damage stages. It should be noted that beams 2 and 3 are loaded at a later age than beam 1. This fact explains their higher E-modulus of beams 2 and 3. From Tables 2–4, it can be shown that the difference between the finite element results and the measured natural frequencies is in general less than 1%. This means that the beam model represents the measurement quite well and can be used with confidence for future damage detection after each load step.

TABLE 2

Natural frequencies of beam 1—reference test—$EI = 55{\cdot}6 \times 10^5$ N m^2, $\rho = 2500$ kg/m^3

Mode	1	2	3	4
Measured	20·67	56·89	109·6	180·7
F.E.	20·79	56·91	110·45	180·24
% difference	0·5	0·03	0·7	0·2

TABLE 3

Natural frequencies of beam 2—reference test—$EI = 66{\cdot}3 \times 10^5$ N m^2, $\rho = 2500$ kg/m^3

Mode	1	2	3	4
Measured	22·47	62·66	120·1	198·9
F.E.	22·68	62·09	120·51	196·66
% difference	0·9	0·9	0·3	1·1

TABLE 4

Natural frequencies of beam 3—reference test—$EI = 63{\cdot}3 \times 10^5$ N m^2, $\rho = 2500$ kg/m^3

Mode	1	2	3	4
Measured	21·9	60·3	117·0	192·0
F.E.	22·16	60·66	117·74	192·13
% difference	1·1	0·6	0·6	0·06

The updating algorithm described in Section 2 is now applied to the different beams at the different load steps. In transferring the damage function into the finite elements, a constant E-modulus is assumed over an element. The error introduced due to the drop in E-modulus between two successive elements will be reduced as the mesh is refined. Another way to implement the damage function, is to define a linear bending stiffness variation along an element length. For the 30-element model, both techniques have produced similar results. The natural frequencies of the four bending modes are used as modal parameters (vector $\mathbf{z}$) in the updating algorithm. The three damage parameters β, α and n are considered as updating parameters (vector $\boldsymbol{\theta}$) making a 4×3 sensitivity matrix ($[\mathbf{S}]_{4\times 3}$). It should be noted that mode shapes have been also considered in a modal parameter vector for some load steps using weighting factors. The ratio between the weighting factors for the mode shapes and those of the frequencies was about 10%. In this case, the dimensions of the sensitivity matrix become 252×3 ((4 natural frequencies + 4 modes $\times$ 62 displacement mode shapes) $\times$ 3 updating parameters). No noticeable difference was observed in the results when the mode shapes are included in the updating algorithm. These results can be explained by two reasons. The first one is that the natural frequencies are more sensitive to damage than the mode shapes. The second reason is that the frequencies are weighted more than the mode shapes in the updating algorithm.

The updating algorithm has been always converged after few iterations. For beams 1 and 2, β is limited to 0·6 and for beam 3–1·0, corresponding to the distance between the two supports. For beam 1, β is converged to 0·6 from the first load step. α decreases from 0·73 (27% damage) at the first load step to 0·5 (50% damage) at the last load step. n increases from 0·59 at load step 1 up to 0·98 at failure. The evolution of damage pattern for beam 1 is illustrated in Figure 7.

For beam 2, it was found that the β value for load step 2 (0.55) is higher than that for load step 3, which is physically impossible. In fact, for load step 2, $\beta \times 30/2$ equals 8·25 elements and for load step 3 is 7·875. This means that for both cases 8 elements are damaged. From load steps 4–7, β reaches 0·6. α varies from 0·85 (15% damage) at load step 1 to 0·49 (51% damage) at load step 7. n is converged to values between (0.533 and 0·84. The progress of damage at the seven load steps of beam 2 is shown in Figure 8.

For beam 3, β is converged to about 1·0 at the third load step indicating that the whole beam is already damaged. α varies from 0·85 (15% damage) at step 1 up to 0·49 (51% damage) at step 6. n is converged to values between 1·4 and 2·2. Figure 9 shows the evolution of damage along the beam length for the different load steps.

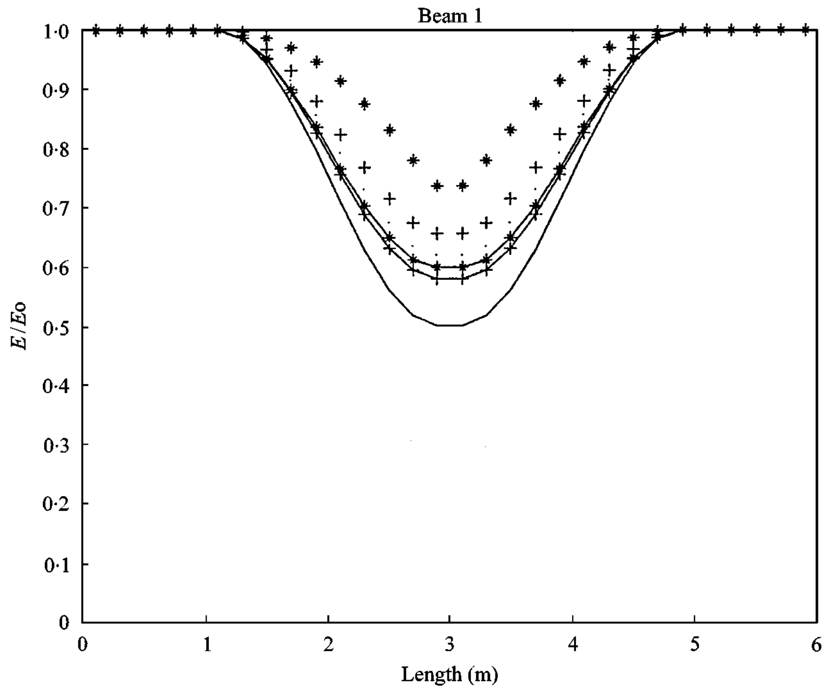

Figure 7. Damage patterns for beam 1. ✱, step 1; + +, step 2; · ·, step 3; ✱—✱, step 4; +——+, step 5; ——, step 6.

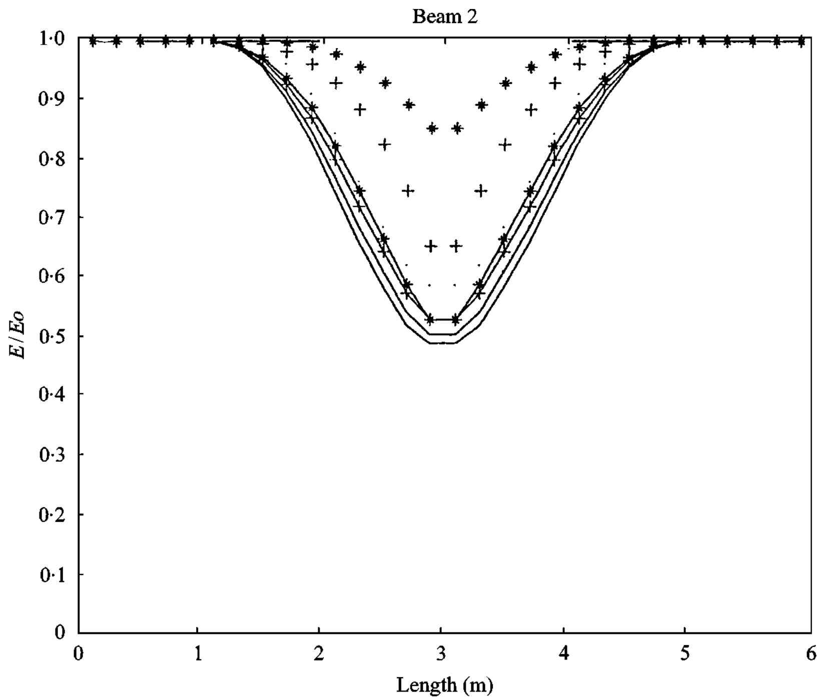

Figure 8. Damage patterns for beam 2. ✱, step 1; + +, step 2; · ·, step 3; ✱—✱, step 4; +——+, step 5; ——, step 6; ——, step 7.

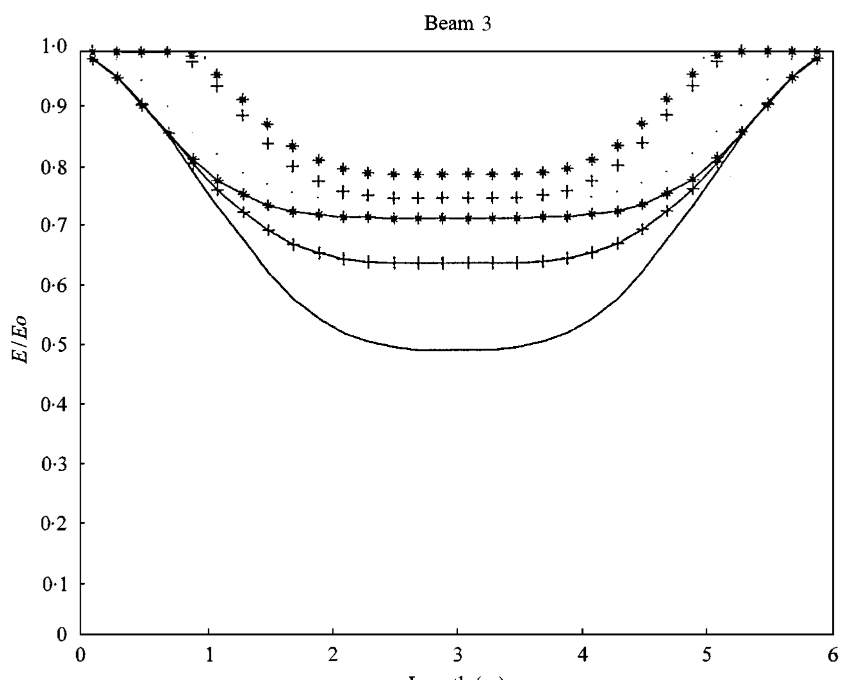

Figure 9. Damage patterns for beam 3. ✱, step 1; + +, step 2; · ·, step 3; ✱—✱, step 4; +——+, step 5; ——, step 6.

It should be noted that during the experimental measurements, the beam was visually inspected after each load step in order to identify the damage zone length and the crack sizes. It was observed that at the second load step, all cracks along the distance between the two supports were already initiated. At the next steps, the crack opening was increasing. These observations agree very well with the updating results in Figures 7–9.

7. CONCLUSIONS

Three laboratory reinforced concrete beams were subjected to static load up to failure in different steps. One concentrated load was applied to the first two beams while two concentrated loads to the third one. The modal parameters of the beams were measured after each load step. A finite element modal-updating algorithm has been developed and implemented. A new concept for damage parameterization in reinforced concrete structures has been presented. A damage function has been proposed in order to describe the damage pattern. By updating three parameters (β, α and n), the damage pattern and its magnitude were successfully determined after each load step.

ACKNOWLEDGMENT

This work was carried out in the framework of FWO-project No. G.0243.96.

REFERENCES

1. P. Cawley and R. D. Adams 1979 *Journal of Strain Analysis* **4**, 49–57. The location of defects in structures from measurements of natural frequencies.
2. O. S. Salawu 1997 *Journal of the British Institute of Non-Destructive Testing* **39**, An integrity index for structural assessment of engineering structures using modal testing.
3. Z. Uzgider, A. K. Sanli , F. Piroglu and D. B. Caglayan 1993 *Bridge Management* 2 (J. E. Harding, G. A. R. Parke and M. J. Ryall, editors), 833–841 London: Thomas Telford. Identification of railway bridges using locomotive-induced vibrations.
4. K. Y. Zhang, A. J. Gu and J. W. Li 1992 *Proceedings of the* 10*th International Modal Analysis Conference*, *San Diego*, *CA*. 549–553. Diagnosis of a slot fault on a frame structure.
5. K. Y. Zhang, L. J. Cheng and T. X. Jin 1993 *Proceedings of the* 11*th International Modal Analysis Conference*, *Kissimmee*, FL. 690–695. Research on the diagnosis of defect on a building foundation piles.
6. J. E. Mottershead and S. James 1997 *Proceedings of the Third International Conference on Modern Practice in Stress and Vibration Analysis*, *Dublin*, *Ireland*. 227–232. The modelling of a three-story aluminium space frame and updating of finite element parameters at the joints.
7. M. M. Abdel Wahab, G. De Roeck, B. Peeters, J. De Visscher, W. P. DE Wilde, G. Van Vinckenory, J.-M. Ndambi and J. Vantomme 1998 *Proceedings of ICES*98, *Atlanta*, *GA*, 6–9 October. Damage evaluation of a reinforced concrete beam using finite element model updating.
8. J. D. Collins, G. C. Hart, T. K. Hasselman and B. Kennedy 1973 *American Institute of Aeronautics and Astronautics Journal* **12**, 185–190. Statistical identification of structures.

9. J. D. Collins, J. Young and L. Kiefling 1972 *Annual Meeting of ASME* 45–71. Methods and applications of system identification in shock and vibration.
10. M. I. Friswell 1989 *Mechanical System and Signal Processing* **3**, 143–155. The adjustment of structural parameters using minimum variance estimator.
11. D. T. Grossman 1982 23*rd Structural Dynamic and Material Conference*, Vol. 2, 68–76. An automated technique for improving modal test/analysis correlation.
12. E. Dascotte 1990 *Eighth IMAC*, 1032–1037. Practical applications of finite element tuning using experimental modal data.
13. K. Kochersbergen, L. D. Mitchell and A. L. Wicks 1992 *Proceedings of the* 10*th IMAC*, 375–381. An efficient method for determining magnitude and phase from laser velocimeter.
14. J. R. F. Arrunda, F. Sun and L. D. Mitchell 1992 *Proceedings of the* 10*th IMAC*, 656–664. Spatial domain techniques for modal analysis using a laser Doppler velocimeter.
15. O. S. Salawu 1995 *Journal of the British Institute of Non-Destructive Testing*, **37**, 875–878. Non-destructive assessment of structures using the integrity index method applied to a concrete highway bridge.
16. C. Williams and O. S. Salawu 1994 *Bridge Assessment Management and Design*, (B. I. G. Barr *et al*., editors), London: Elsevier. Concepts of condition assessment of bridges using vibration testing and analysis.
17. C. Sikorsky and N. Stubbs 1997 *Structural Damage Assessment Using Advanced Signal Processing Procedures*, 399–408. Sheffield University Press. Improving bridge management using NDT and quality management.
18. C. Farrar and D. Jauregai 1996 *Technical Report*, *LA*-13074-*MS*, *Los Alamos*, *National Laboratory*. Damage detection algorithms applied to experimental and numerical modal data from the 1–40 bridge.
19. C. E. Ventura and P. Adebar 1997 *Proceedings of the International Modal Analysis Conference—IMAC*, Vol. 2, 1103–1109. Modal properties and damage detection of a concrete-steel hybrid girder bridge.
20. K. Krishnan, F. Seible and G. Pardoen 1996 *Structures Congress—Proceedings*, Vol. 2, 845–852. Evaluation of bridge strengthening measures using forced vibration tests.
21. M. M. Abdel Wahab and G. De Roeck 1999 *Journal of Sound and Vibration*. Damage detection in bridges using modal curvatures: Application to a real damage scenario. to appear.
22. P. Gill, W. Murray and M. Wright 1981 *Practical Optimisation*. San Diego. Academic Press.
23. M. I. Friswell and J. E. Mottershead 1995 *Finite Element Model Updating in Structural Dynamics*. Dordrecht, The Netherlands: Kluwer Academic Publisher.
24. S. M. Pandit 1991 *Modal and Specturm Analysis*: *Data Dependent Systems in State Space*. New York Wiley.
25. P. Van Overschee and B. De Moor 1991 30*th IEEE Conference on Decision and Control*, *Brighton*, *UK*, pp. 1321–1326. Subspace algorithms for the stochastic identification problem.